Journal of Veterinary Internal Medicine
Open Access
ACVIM American College of Veterinary Internal Medicine

J Vet Intern Med 2015;29:1354–1359

Low-Field Magnetic Resonance Imaging and Multislice Computed Tomography for the Detection of Cervical Syringomyelia in Dogs

K. Kromhout, H. van Bree, B.J.G. Broeckx, S. Bhatti, S. De Decker, I. Polis, and I. Gielen

Background: Syringomyelia (SM) is defined as the presence of fluid-containing cavities within the parenchyma of the spinal cord. Sagittal magnetic resonance (MR) images have been described as the preferred technique for visualizing SM in dogs and humans.

Objective: To investigate whether computed tomography (CT) can be used to diagnose SM.

Animals: Thirty-two client-owned dogs referred for investigation of the cervical spine on magnetic resonance imaging (MRI) and CT.

Methods: Two reviewers retrospectively analyzed sagittal and transverse T1-weighted spin echo (T1WSE) MR images and CT images from each dog for the presence of SM and, if SM was present, the width (mm, syrinx width [SW]) was measured. The results were analyzed statistically.

Results: For the presence of SM there was a moderate interobserver agreement for MR (81%, $\kappa = 0.54$) and almost perfect agreement for CT (94%, $\kappa = 0.87$). There was a moderate intramodality agreement for both observers (observer 1 81%, $\kappa = 0.59$; observer 2 81%, $\kappa = 0.57$). For measurement of SW the repeatability was the best on the midsagittal T1WSE images (95% repeatability coefficient <0.52 mm) and the reproducibility was the best on midsagittal images in both modalities (95% limits of agreement −0.55–0.45; $P = 0.002$).

Conclusion and Clinical Importance: Both techniques can be used to detect SM. Midsagittal MR and CT images are best used for measuring SW. Computed tomography can be used as a diagnostic tool for SM when MRI is not available, but CT cannot replace MRI as the standard screening technique for the detection of SM in Cavalier King Charles Spaniel for breeding purposes.

Key words: Axial imaging modalities; Cavalier King Charles Spaniels; Syrinx.

Syringomyelia (SM) is a condition characterized by the development of fluid-containing cavities in the spinal cord.[1] The fluid in the cavities resembles cerebrospinal fluid but has a lower protein content.[2,3] Syringomyelia has been considered as a rare disease in veterinary medicine, but is more and more recognized in animals because of the increased availability of magnetic resonance imaging (MRI) and the increased prevalence in certain breeds such as Cavalier King Charles spaniels (CKCS),[4] Griffon Bruxellois[5], and other small or 'toy' breeds.[6] One of the most common causes in dogs is Chiari-like malformation in CKCS.[1,7,8] In this disorder there is a mismatch between the caudal cranial fossa volume and brain parenchyma which leads to cerebellar herniation, medullary kinking, obstruction of the dorsal craniocervical subarachnoid space, and alteration of the cerebrospinal fluid flow.[7] Other causes of SM in dogs include trauma,[9,10] caudal fossa masses[11], and hydrocephalus.[12]

Abbreviations:

CKCS	Cavalier King Charles Spaniel
CT	computed tomography
MRI	magnetic resonance imaging
SM	syringomyelia
SW	syrinx width
T1WSE	T1-weighted spin echo
T2WSE	T2-weighted spin echo

Magnetic resonance imaging is mentioned in several articles in human and veterinary medicine as the preferred imaging technique for visualizing changes in the spinal cord and to detect SM.[1,13–16] However, plain computed tomography (CT) and CT after intrathecal injection of nonionic contrast media have also been used in human medicine to detect SM.[16] Studies on the comparison of these imaging modalities for the detection of SM are not yet available in veterinary medicine. The goal of this study was therefore to retrospectively evaluate the agreement within and between sagittal and transverse low-field MRI and multislice CT for the detection of SM and measurement of syrinx width (SW) in dogs.

Materials and Methods

Subjects

This retrospective study included client-owned dogs that were evaluated through the Department of Veterinary Medical Imaging

From the Department of Veterinary Medical Imaging and Small Animal Orthopedics, Faculty of Veterinary Medicine, Ghent University, Ghent, Belgium (Kromhout, van Bree, Gielen); the Laboratory of Pharmaceutical Biotechnology, Faculty of Pharmaceutical Sciences, Ghent University, Ghent, Belgium (Broeckx); the Department of Small Animal Medicine and Clinical Biology, Faculty of Veterinary Medicine, Ghent University, Ghent, Belgium (Bhatti, Polis); and the Department of Clinical Science and Services, Royal Veterinary College, University of London, London, UK (De Decker).

This work was done at the Department of Veterinary Medical Imaging and Small Animal Orthopedics, Faculty of Veterinary Medicine, Ghent University, Salisburylaan 133, 9820 Merelbeke, Belgium.

Corresponding author: K. Kromhout, Department of Veterinary Medical Imaging and Small Animal Orthopedics, Faculty of Veterinary Medicine, Ghent University, Salisburylaan 133, 9820 Merelbeke, Belgium; e-mail: kaatje.kromhout@ugent.be.

Submitted January 27, 2015; Revised April 13, 2015; Accepted June 11, 2015.

DOI: 10.1111/jvim.13579

and Small Animal Orthopedics of the Faculty of Veterinary Medicine, Ghent University, between January 2012 and August 2014. After medical histories were obtained and a complete clinical evaluation including a general physical and neurologic examination was performed, the dogs underwent (as part of their clinical work-up) both MRI and CT studies of the cervical region. Thirty-two dogs were included in the study. Dog breeds were CKCS (n = 12), French Bulldog (n = 7), Maltese dogs (n = 2), Border Collie (n = 2), Bordeaux Dog (n = 2) and one each of the following: Shi Tzu, Chihuahua, Yorkshire Terrier, English Springer Spaniel, Jack Russell Terrier, Rottweiler, and Galgo Espanol. Among dogs, 17 were female and 15 were male. The mean age was 63 months (range 6–144 months) in the dogs. Clinical signs detected or reported by owners at the initial evaluation varied, the most common of which were neck pain, ataxia, and tetraparesis.

Magnetic Resonance Imaging Protocol

Imaging was performed using a 0.2 Tesla MRI unit.[a] The animals were anesthetized and positioned in dorsal recumbency, with the area of interest placed in a human neck/cervical spine coil or a quadrature flexible spine/body coil used in human medicine. Protocols included precontrast sagittal and transverse T1-weighted spin echo (T1WSE) imaging and T2-weighted spin echo (T2WSE) imaging in the same planes. Four-millimeter-thick contiguous slices were chosen (image matrix, 512 × 512).

Computed Tomography Protocol

Imaging was performed using a four-slice helical CT device.[b] The animals were anesthetized and positioned in dorsal recumbency. Images in 1.25-mm-thick contiguous slices (120 kVp, 140 mAs, image matrix 512 × 512) were obtained, before and immediately after administration of 2 mL/kg (600 mg Iodine/kg body weight) intravenous iodinated contrast medium (Ultravist 300 (300 mg Iodine/mL); N.N. Shering S.A.). The raw data were reconstructed in soft tissue algorithm.

Imaging Analysis

Before analysis, MR and CT images were loaded into open source imaging software.[c] Images were blinded, randomized, and independently evaluated by two experienced observers (KK and IG). All CT images were reviewed in a brain window. Adjustments of the window width and level were made by the radiologists individually to allow better visualization. Syringomyelia was defined by the presence of an intramedullary fluid filled cavity with uniform signal intensity and density identical to cerebrospinal fluid (T1WSE: hypointense to spinal cord parenchyma; CT: hypodens to spinal cord parenchyma) in the ventricular system. The presence of SM on the MRI and CT images was noted as absent or present.

Morphometric Procedure

In case SM was present, the maximal dorsoventral SW (Fig 1) was measured perpendicular to the longitudinal axis of the spinal cord on the midsagittal images and by measuring the widest dorsoventral diameter of the syrinx on the transverse images at the same level. Different planes in both modalities were used for the measurements: midsagittal and transverse T1WSE MR images and postcontrast transverse and midsagittal 2D multiplanar reformatted CT images.

Statistical Analysis

Statistical analyses were performed in R.[17] The analysis was subdivided in the assessment of the agreement for a categorical

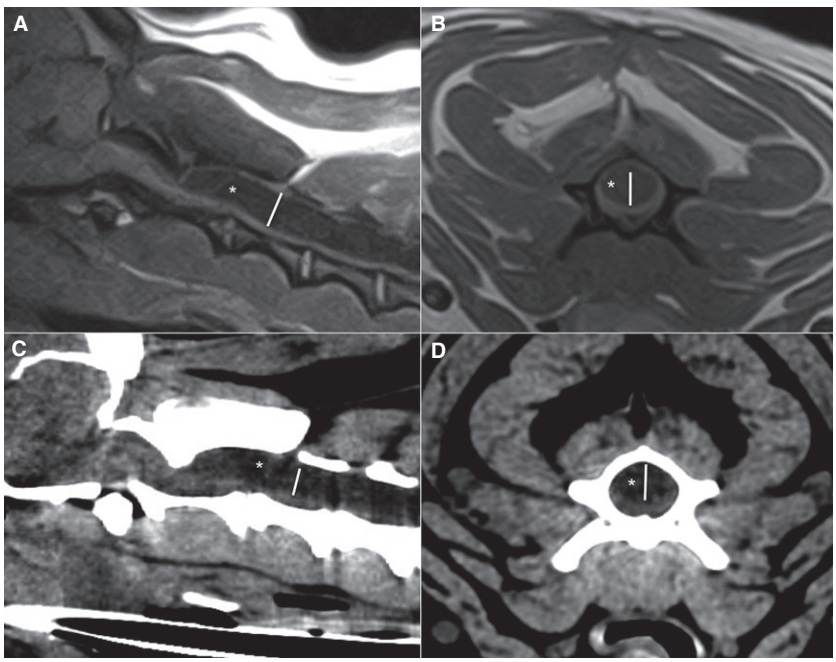

Fig 1. Midsagittal (**A**) and transverse (**B**) T1-weighted spin echo image and corresponding midsagittal (**C**) and transverse (**D**) computed tomography images of the cranial cervical spine of the same dog. A hypointense (**A,B**) or hypodens (**C,D**) cavity (white asterisk) is visible within the spinal cord. The syrinx width (white line) is measured perpendicular to the longitudinal axis of the spinal cord on the midsagittal images. On the transverse images the widest diameter (white line) at the same level is measured.

variable (the presence or absence of a syrinx) and a continuous variable (SW).

All dogs (n = 32) were included to assess the agreement on determining the presence or absence of a syrinx, For this diagnosis, each observer had access to both the sagittal and transverse plane from the same modality (CT or MR). To determine the repeatability, one observer assessed each dog twice with a 2-week interval between the assessments, for both CT and MR (=intraobserver intramodality agreement). To determine the reproducibility within a modality (CT or MR), the diagnosis from both observers was compared (interobserver intramodality agreement). To determine the reproducibility between modalities for each individual observer, the diagnosis from each observer was compared for CT and MR (intraobserver intermodality agreement). For each analysis, the overall agreement (dogs with agreement divided by total number of dogs) and a kappa statistic were calculated.[18]

Only dogs, where the agreement on the presence of a syrinx was unanimous for both imaging modalities, were used to assess the agreement on the measurement of the SW. This ensures the observed differences are not caused by a different number of dogs or by the in- or exclusion of specific dogs. Hence, all values can be compared directly. To determine the repeatability, each dog was measured three times by one observer. Using these results, the 95% repeatability coefficient was calculated as suggested by Bland and Altman[19] (intraobserver intramodality intraplanar agreement). To determine the reproducibility, the mean difference (a measurement for systematic bias) and the 95% limits of agreement were calculated.[19] A paired Student's *t*-test was performed to determine whether the systematic bias was significantly different from zero. Three different comparisons were made. First, the reproducibility within one plane and modality (=interobserver intramodality intraplanar agreement) for two different observers was assessed. Next, the agreement within one modality between planes for two different observers was assessed (=interobserver intramodality interplanar agreement). Finally, the agreement for two different observers between modalities within a plane (=interobserver intermodality intraplanar agreement) was calculated.

Results

Detection of Syrinx

Repeatability and Reproducibility. There was a perfect intraobserver intramodality agreement for detection of a syrinx on CT and MR images in consecutive viewings (Table 1). There was a moderate interobserver intramodality agreement for MR and almost perfect agreement for CT on the detecting of a syrinx. There was a moderate intraobserver intermodality agreement for both observers.

Table 1. Agreement between magnetic resonance imaging (MRI) and computed tomography (CT) and observers for the detection of a syrinx (total n examined = 32).

	κ	% of Agreement
Repeatability		
Intraobserver intramodality		
MRI	1	100
CT	1	100
Reproducibility		
Interobserver intramodality		
MRI	0.54	81
CT	0.87	94
Intraobserver intermodality		
Observer 1	0.59	81
Observer 2	0.57	81

κ, Kappa value; levels of agreement: almost perfect ($0.8 < \kappa \leq 1$), substantial ($0.6 < \kappa \leq 0.8$), moderate ($0.4 < \kappa \leq 0.6$), fair ($0.2 < \kappa \leq 0.4$), slight ($0.2 < \kappa \leq 0$).

Table 2. Reproducibility agreement between MRI and CT for the measurement of syrinx width (total n examined = 17).

	Bias	*P*-value	95% LOA (lower to upper limit)	SD
Interobserver intramodality intraplanar agreement				
Midsagittal T1WSE	−0.09	<0.01	−0.25 to 0.06	0.08
Transverse T1WSE	−0.052	0.029	−0.23 to 0.13	0.09
Transverse CT	−0.041	0.16	−0.27 to 0.19	0.12
Midsagittal CT	−0.063	0.046	−0.30 to 0.18	0.12
Interobserver intramodality interplanar agreement				
Midsagittal & transverse T1WSE	−0.043	<0.01	−0.53 to 0.45	0.25
Midsagittal & transverse CT	−0.0043	0.62	−0.52 to 0.51	0.26
Interobserver intermodality intraplanar agreement				
Midsagittal T1WSE & CT	−0.049	0.002	−0.55 to 0.45	0.26
Transverse T1WSE & CT	−0.01	0.61	−0.55 to 0.53	0.28

MRI, magnetic resonance imaging; CT, computed tomography; T1WSE, T1-weighted spin echo; SD, standard deviation; LOA, limits of agreement.

Measurement of Syrinx Width

Repeatability. As determined by the 95% repeatability coefficient, 95% of 3 consecutive readings of SW will be within 0.52 mm for the T1WSE midsagittal images, 0.60 mm for the midsagittal CT images, 0.61 mm for the T1WSE transverse, and 0.62 mm for the transverse CT images.

Reproducibility. (A) Interobserver intramodality intraplanar agreement

A systematic bias significantly different from zero was identified for measuring SW on T1WSE midsagittal, T1WSE transverse images, and midsagittal CT images between the observers (Table 2). There was no significant difference present for measuring SW on transverse CT images between the observers. The reproducibility was highest for midsagittal T1WSE, followed by transverse T1WSE, transverse CT, and midsagittal CT.

(B) Interobserver intramodality interplanar agreement

A bias significantly different from zero was identified for measuring the SW between T1WSE midsagittal and transverse images. No significant difference was identified for measurements between midsagittal and transverse CT images. Magnetic resonance images had the highest reproducibility.

(C) Interobserver intermodality intraplanar agreement

The bias was significantly different from zero for the measurement of SW between T1WSE midsagittal and midsagittal CT images and no significant difference in between T1WSE transverse and transverse CT images. The midsagittal images over modalities had the highest reproducibility.

Discussion

Results of this study demonstrate that low-field MR and multislice CT imaging provide comparable information regarding the presence of SM. Analyses of the intraobserver repeatability resulted in the best repeatability for measurement of SW on the midsagittal images (T1WSE > CT) and the least on transverse images (T1WSE > CT). An almost similar result was obtained for the interobserver reproducibility.

Significant bias was identified in some comparisons, This is no issue, however, as this indicates the systematic differences between modalities/observers or planes. A systematic difference can be easily corrected by subtracting or adding this bias to the results from one technique, to obtain the values for the other technique. A bigger issue is a large standard deviation (and consequently large limits of agreement) as they indicate a nonsystematic difference and cannot be corrected for.

For the diagnosis and morphometric studies of SM, MR is the imaging modality of choice both in human and veterinary studies, because of its high contrast resolution and multiplanar capabilities. This was also reflected in the results of this study. Thin section images should be obtained to limit partial volume effects and allowing optimal visualization of small syrinx cavities. In human medicine, most of the investigations concerning SM have been carried out on T1WSE images.[20,21] Veterinary studies have used T2WSE images[13,22] and T1WSE images[8,14,23] to evaluate SM. T1-weighted spin echo images were used for the measurements in this study. Measurements of the syrinx on T2WSE images may result in an overestimation of the size because the borders of the syrinx are not well demarcated[23] as they can include the hyperintense signal associated with interstitial edema. This interstitial edema or presyrinx state[20,24] is an accumulation of fluid in the parenchyma before syrinx formation. In addition, several artifacts interfere more on T2WSE images compared with T1WSE images. Two such artifacts are the truncation and susceptibility artifact. Truncation artifact is a common source of high signal intramedullary bands on midsagittal T2WSE images which can be mistaken for a syrinx.[25] Susceptibility artifacts because of metallic foreign bodies, such as ID microchips in veterinary patients, are commonly seen on MR images of the cervical spine. These are more obvious on T2WSE images and cause a distortion of the spinal cord on this level which may influence the detection of SM in the cervical spine.[26] Computed tomography is not routinely used to investigate intramedullary changes because of the lesser contrast resolution compared with MRI. Images from plain CT are considered unreliable because of the imaging distortions of the surrounding bone (beam artifact).[27] This artifact is more pronounced in past generation CT scanners. Multislice CT scanners, such as the one used in this study, can reduce these artifacts and provide better temporal and contrast resolution. An advantage of CT compared with MRI is the ability to acquire thin slices without loss of detail on the reformatted images and a high signal to noise ratio in contrast to MRI where thinner slices result in a decrease in detail and a decreased signal to noise ratio. In our study a different slice thickness has been used for both modalities (MRI = 4 mm; CT = 1.25 mm) to optimize the visualization of the spinal cord. Optimal CT and MRI imaging parameters, including slice thickness, for the cervical spine have already been established in previous articles.[28,29] We are aware that the small CT slice thickness used during our examinations can be different from the thickness that is used standard in other clinics and can influence the detection of SM in those cases.

Previous articles have stated that CT only allows detection of large intramedullary cavities. Smaller cavities are only seen if they fill with contrast (=CT myelography).[30] Computed tomography myelography is able to show swelling and fixation of the spinal cord and localized cerebrospinal fluid flow obstruction.[27] A syrinx is identified by delayed accumulation of water-soluble contrast within the spinal cord in <4 hours. In human medicine, 10–50% of syrinxes are not detected using CT myelography.[31] In addition, this technique is invasive and is reported to cause adverse effects such as seizures or neurological deterioration.[32] Consequently and because of the infrequent use of CT myelography in our clinic, this technique was not used in this study.

When we look at the differences in measurements between the different planes in MR and CT images and between the modalities there is a significant mean difference between the transverse and midsagittal planes in MR and the midsagittal planes between MR and CT. The discrepancy between the SW on midsagittal and transverse MR images can be attributed to the fact that we choose midsagittal images based on the visualization of the spinous process to assure that the measurements were made at the maximum diameter of the spinal canal and cord. This can be off midline (Fig 2) resulting in a different width compared with the transverse images. Furthermore the large thickness of the slices on MR compared to the size of the cervical spinal cord can also produce off midline images. This might also (partially) explain the differences between the midsagittal MR and CT images. With CT, we can work with reformatted and smaller thickness images where we can create images almost exact in the midline. The common definition of a syrinx is the presence of a fluid-containing cavity within the spinal cord parenchyma with a diameter ≥2 mm at his widest point.[13] This is also the cut-off value that is used in the breeding recommendations of CKCS.[33] The central canal is normally just appreciable on MR images and not visible in normal circumstances on CT images. However, any dilatation of the central canal should be considered abnormal. Hence, the detection of smaller dilatations on both MR and CT is important as progres-

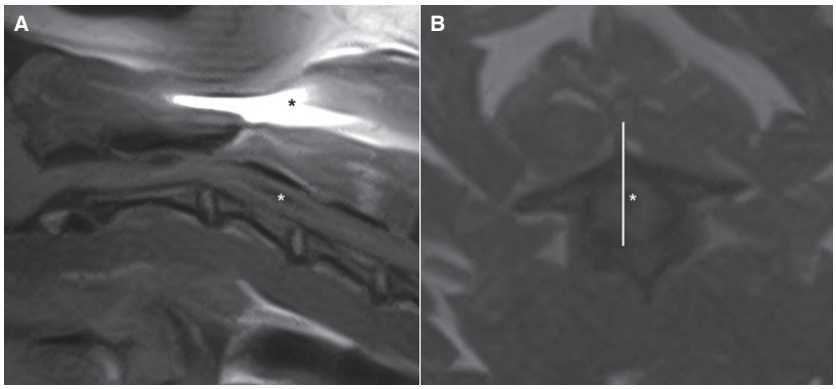

Fig 2. Midsagittal (**A**) and transverse (**B**) T1-weighted spin echo image of the cranial cervical spine of the same dog. A hypointense cavity (white asterisk) is visible within the spinal cord. A susceptibility artifact (*) is visible because of the presence of a microchip. The corresponding slice (white line) of the sagittal image is off midline compared to the transverse image.

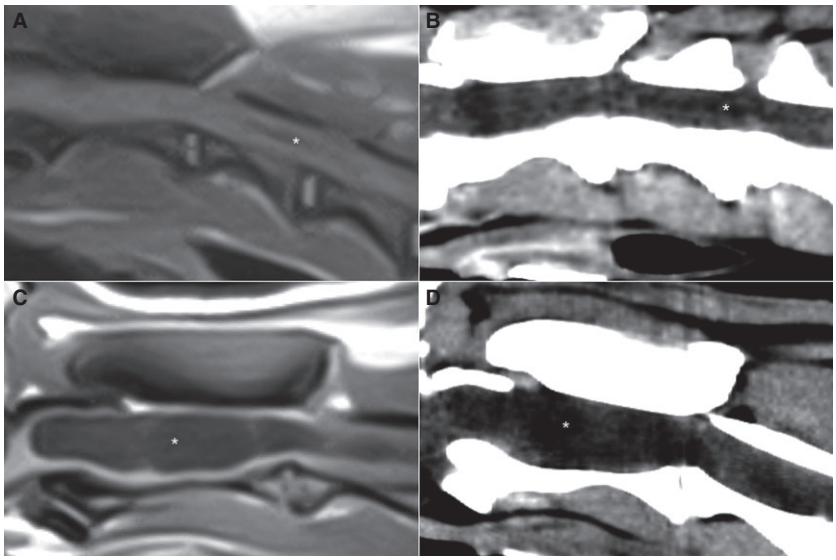

Fig 3. Midsagittal (**A**) T1-weighted spin echo (T1WSE) and corresponding (**B**) computed tomography (CT) image of the cranial cervical spine of dog 1 and midsagittal (C) T1WSE and corresponding (D) CT image of the cranial cervical spine of dog 2. (**A,B**) A small (<1.5 mm, white asterisk) dilatation of the central canal is visible and (**C,D**) a large (>4 mm, white asterisk) syrinx is visible.

sive central canal dilatation is a precursor of syrinx formation.[1,34] Furthermore, results of a previous study suggest that SW progresses with time in CKCS.[34] Syrinx width has been shown to be the strongest predictor of pain in CKCS. A syrinx of >6.4-mm wide causes clinical signs in 95% of CKCS.[12] In a study conducted in American Brussels Griffon dogs, there was no association found between the size and pain, only between size (>1 and <2 mm) and Chiari malformation signs.[35] Also in human medicine signs of pain are not well correlated with the size of the syrinx. Damage to the dorsal horn of the spinal cord is a key feature in the presence of pain.[36] Further studies have to be conducted in other breeds to see if the size of a syrinx has an effect on the clinical signs in these dogs. This study did not find an association between the detection of a small dilatation and use of technique (Fig 3). The difference in detection and measurement can be attributed to the experience of the observer and the presence of several of the artifacts mentioned earlier. Overall, we conclude that SM is consistently identified by different observers on CT and on MRI. In addition, the results of this study suggest that when a syrinx is detected the highest agreement is present for measuring SW on both the midsagittal MR and CT images. Syringomyelia and SW have been shown to explain at least some of the clinical signs in dogs. As CT scanners are more readily available in veterinary practices compared with MRI equipment, CT can be used as a diagnostic tool for SM when MRI is not available. Cerebellar herniation is consistently identified by different observers on CT and on MR images of CKCS.[37] Bearing this in mind, we can conclude, that CT can be used as an alternative imaging technique for Chiari-like malformation/SM in CKCS when MRI is not available. We emphasize that, at the current time, CT cannot replace MRI as the standard screening technique for the detection of SM in CKCS for breeding purposes, more specific for the detection of the presyrinx state.[20,24]

Footnotes

[a] Airis Mate, Hitachi, Japan
[b] Lightspeed Qx/i, General Electric Medical Systems, Milwaukee, WI
[c] OsiriX Medical Imaging Software version 4.1.2 DICOM viewer, Pixmeo, Bernex, Switzerland

Acknowledgments

Funding: No funding.

Conflict of Interest Declaration: Authors disclose no conflict of interest.

Off-label Antimicrobial Declaration: Authors declare no off-label use of antimicrobials.

References

1. Rusbridge C, Greitz D, Iskandar BJ. Syringomyelia: Current concepts in pathogenesis, diagnosis, and treatment. J Vet Intern Med 2006;20:469–479.

2. Levine DN. The pathogenesis of syringomyelia associated with lesions at the foramen magnum: A critical review of existing theories and proposal of a new hypothesis. J Neurol Sci 2004;220:3–21.

3. Greitz D. Unraveling the riddle of syringomyelia. Neurosurg Rev 2006;29:251–263.

4. Cross HR, Cappello R, Rusbridge C. Comparison of cerebral cranium volumes between Cavalier King Charles spaniels with Chiari-like malformation, small breed dogs and Labradors. J Small Anim Pract 2009;50:399–405.

5. Rusbridge C, Knowler SP, Pieterse L, et al. Chiari-like malformation in the Griffon Bruxellois. J Small Anim Pract 2009;50:386–393.

6. Dewey C, Berg J, et al. Foramen magnum decompression for treatment of caudal occipital malformation syndrome in dogs. J Am Vet Med Assoc 2005;227:1270–1275.

7. Driver CJ, Volk HA, Rusbridge C, Van Ham LM. An update on the pathogenesis of syringomyelia secondary to Chiari-like malformations in dogs. Vet J 2013;198:551–559.

8. Parker JE, Knowler SP, Rusbridge C, et al. Prevalence of asymptomatic syringomyelia in Cavalier King Charles spaniels. Vet Rec 2011;168:667.

9. Olby N. The pathogenesis and treatment of acute spinal cord injuries in dogs. Vet Clin North Am Small Anim Pract 2010;40:791–807.

10. Feliu-Pascual AL, Garosi L, Dennis R, et al. Iatrogenic brainstem injury during cerebellomedullary cistern puncture. Vet Radiol Ultrasound 2008;49:467–471.

11. da Costa RC, Parent JM, Poma R, et al. Cervical syringohydromyelia secondary to a brainstem tumor in a dog. J Am Vet Med Assoc 2004;225:1061–1064.

12. Kitagawa M, Ueno H, Watanabe S, et al. Clinical improvement in two dogs with hydrocephalus and syringohydromyelia after ventriculoperitoneal shunting. Aust Vet J 2008;86:36–42.

13. Rusbridge C, Carruthers H, Dubé MP, et al. Syringomyelia in Cavalier King Charles spaniel: The relationship between syrinx dimensions and pain. J Small Anim Pract 2007;48:432–436.

14. Couturier J, Rault D, Cauzinille L. Chiari-like malformation and syringomyelia in normal Cavalier King Charles spaniels: A multiple diagnositic imaging approach. J Small Anim Pract 2008;49:438–443.

15. Kirberger RM, Jacobson LS, Davies JV, et al. Hydromelia in the dog. Vet Radiol Ultrasound 1997;39:30–38.

16. Doyon D, Benoudiba F, Iffenecker C, et al. Imaging of syringomyelia. Neurochirurgie 1999;45:105–114.

17. R Core team. R: A Language and Environment for Statistical Computing. Vienna, Austria: R Foundation for Statistical Computing; 2012. ISBN 3-900051-07-0, URL http://www.R-project.org/.

18. Landis JR, Koch GG. The measurement of observer agreement for categorical data. Biometrics 1977;33:159–174.

19. Bland JM, Altman DG. Measuring agreement in method comparison studies. Stat Methods Med Res 1999;8:135–160.

20. Akiyama Y, Koyanagi I, Yoshifuji I, et al. Interstitial spinal-cord oedema in syringohydromyelia associated with Chiari type 1 malformations. J Neurol Neurosurg Psychiatry 2008;79:1153–1158.

21. Trigylidas T, Baronia B, Vassilyadi M, et al. Posterior fossa dimension and volume estimates in pediatric patients with Chiari i malformations. Childs Nerv Syst 2008;24:329–336.

22. Carruthers H, Rusbridge C, Dube MP, et al. Association between cervical and intracranial dimensions and syringomyelia in the Cavalier King Charles spaniel. J Small Anim Pract 2009;50:394–398.

23. Loderstedt S, Benigni L, Chandler K, et al. Distribution of syringomyelia along the entire spinal cord in clinacally affected Cavalier King Charles Spaniels. Vet J 2011;190:359–363.

24. Fishbein NJ, Dillon WP, Cobbs C, et al. The "Presyrinx" state: A reversible myelopathic condition that may precede syringomyelia. AJNR Am J Neuroradiol 1999;20:7–20.

25. Bou-Haider P, Peduto AJ, Karunaratne N. Differential diagnosis of T2 hyperintense spinal cord lesions: Part A. J Med Imaging Radiat Oncol 2009;52:535–543.

26. Hecht S, Adams WH, Narak J, et al. Magnetic Resonance Imaging susceptibility artifacts due to metallic foreign bodies. Vet Radiol Ultrasound 2011;52:409–414.

27. Klekamp J, Samii M. Syringomyelia: Diagnosis and Management, 1st ed. Berlin: Springer; 2002:195.

28. Drees R, Dennison SE, et al. Computed tomographic imaging protocol for the canine cervical and lumbar spine. Vet Radiol Ultrasound 2009;50:74–79.

29. Dennis R. Optimal magnetic resonance imaging of the spine. Vet Radiol Ultrasound 2011;52(Supp. 1):S72–S80.

30. Lee BCP, Zimmerman RD, Manning JJ, et al. MR imaging of syringomylia and hydromelia. AJNR Am J Neuroradiol 1985;6:221–228.

31. Brodfelt AR, Stoodley MA. Post-traumatic syringomyelia: A review. J Clin Neurosci 2003;10:401–408.

32. Barone G, Ziemer LS, Shofer FS, et al. Risk factors associated with development of seizures after use of iohexol for myelography in dogs: 182 cases (1998). J Am Vet Med Assoc 2002;220:1499–1502.

33. Capello R, Rusbridge C. Report from the Chiari-like malformation and syringomyelia working group round table. Vet Surg 2007;36:509–512.

34. Driver CJ, De Risio L, Hamilton S, et al. Changes over time in craniocerebral morphology and syringomylia in cavalier King Charles spaniels with Chiari-like malformation. BMC Vet Res 2012;8:215.

35. Freeman AC, Platt SR, Kent M, et al. Chiari-like malformation and syringomyelia in American Brussels griffon dogs. J Vet Intern Med 2014;28:1551–1559.

36. Todor DR, Harrison TM, Millport TH. Pain and syringomyelia: A review. Neurosurg Focus 2008;8:1–6.

37. Kromhout K, van Bree H, Broeckx BJG, et al. Low-field MRI and multislice CT for the detection of cerebellar (foramen magnum) herniation in Cavalier King Charles Spaniels. J Vet Intern Med 2015;29:238–242.